

A FINITE ELEMENT METHOD FOR THE ONE-DIMENSIONAL EXTENDED BOUSSINESQ EQUATIONS

M. WALKLEY* AND M. BERZINS

School of Computer Studies, University of Leeds, Leeds LS2 9JT, UK

SUMMARY

A new finite element method for Nwogu's (O. Nwogu, *ASCE J. Waterw., Port, Coast., Ocean Eng.*, **119**, 618–638 (1993)) one-dimensional extended Boussinesq equations is presented using a linear element spatial discretisation method coupled with a sophisticated adaptive time integration package. The accuracy of the scheme is compared to that of an existing finite difference method (G. Wei and J.T. Kirby, *ASCE J. Waterw., Port, Coast., Ocean Eng.*, **121**, 251–261 (1995)) by considering the truncation error at a node. Numerical tests with solitary and regular waves propagating in variable depth environments are compared with theoretical and experimental data. The accuracy of the results confirms the analytical prediction and shows that the new approach competes well with existing finite difference methods. The finite element formulation is shown to enable the method to be extended to irregular meshes in one dimension and has the potential to allow for extension to the important practical case of unstructured triangular meshes in two dimensions. This latter case is discussed. Copyright © 1999 John Wiley & Sons, Ltd.

KEY WORDS: Boussinesq equations; finite element method; adaptive time integration

1. INTRODUCTION

In the nearshore zone accurate prediction of wave activity needs to account for both non-linear and dispersive effects. Important wave processes include diffraction, refraction, shoaling and harmonic interaction. The Boussinesq equations model weakly non-linear, weakly dispersive water waves in a variable depth environment. In shallow water their linearised dispersion characteristics approximate Stokes first-order wave theory [1]. All the Boussinesq equation systems are derived by integrating the higher dimensional fluid flow equations through the depth. This produces a simplified vertical velocity distribution which restricts the validity of the mathematical model to a shallow water environment. The depth integration reduces the spatial dimension of the equations by one and makes them relatively efficient to solve. They are commonly used for predicting wave elevations inside harbours [2,3] and wave interactions in the nearshore zone [4].

The original system of equations proposed by Peregrine [5] are limited to very shallow water; their linearised dispersion characteristics rapidly diverge from the true behaviour in deeper water rendering the model invalid in these situations. In recent years there have been several

* Correspondence to: School of Computer Studies, University of Leeds, Leeds LS2 9JT, UK.

proposals of extended Boussinesq systems for which the dispersion relationship is valid up to the deep water limit, increasing the useful range of these models for many applications. Madsen *et al.* [6] added extra dispersion terms to the original system in order to improve the linear dispersion characteristics. This procedure was extended to a variable depth environment [7], although more recent work by Beji and Nadaoka [8] has suggested that there may be inconsistencies in this approach. Beji and Nadaoka [8] have produced an extended Boussinesq system, valid in a variable depth environment, by a simple algebraic manipulation of Peregrine's original system. In contrast Nwogu [9] derived an extended system of equations from the full fluid equations by choosing the velocity at an arbitrary depth as one of the variables. Although the latter two systems have equivalent linearised dispersion characteristics and shoaling properties, Nwogu's system is used in this work. The proposed finite element method is easier to apply to this form of the equations for reasons given in Section 3.2. Although the extended systems have improved dispersion characteristics, they are all still formally of the same accuracy as the original system and restricted to a shallow water environment.

Most of the numerical schemes for the Boussinesq equations are based on finite difference methods. Abbot *et al.* [2,10] pioneered the finite difference solution of the original Boussinesq system. They showed that careful analysis of the truncation errors was necessary to ensure that an accurate model was obtained. In particular it was shown that the truncation errors of a low-order approximation in space or time could contaminate the real dispersive terms present in the equations. They included the important truncation error terms in their model to prevent this occurring. Nwogu's scheme [9] applied this principle to the extended Boussinesq system. Wei and Kirby [11] eliminated the dispersive errors by differencing selected spatial terms to higher order and integrating in time with a high-order predictor–corrector method. This difference scheme is described in more detail in Section 3.1. The finite difference methods are simple to formulate, but difficulties in modelling irregular geometries in two space dimensions with structured grids can lead to a loss of accuracy [3]. Unstructured finite element methods are straightforward to apply on complex domains but their application in this area has so far been limited to the original Boussinesq system [12–14]. The Diffpack software [15] has also been applied to the original Boussinesq system.

A method of lines approach is adopted in this work. A complete spatial discretisation is performed producing a system of ordinary differential equations in time, and boundary conditions in either algebraic or differential form. This is generally classed as a differential-algebraic equation system. The system is solved using SPRINT [16]; a general purpose time integration package using adaptive order, adaptive time stepping methods driven by state-of-the-art local error control strategies. The aim of this work is to take a first step in the direction of applying finite element methods to geometrically complex two-dimensional problems using unstructured triangular meshes. This will be done by investigating the implementation of finite element methods for the one-dimensional extended Boussinesq equations. Although the spatial discretisation method must have an obvious extension to two-dimensional unstructured triangular grids, at the same time it must be competitive in terms of computational speed with existing finite difference methods. The approach adopted here is to use a linear finite element spatial discretisation coupled with a sophisticated time integration strategy. The linear Galerkin finite element method [17] cannot be applied directly to the system due to the presence of third-order spatial derivatives. Here the equations are rewritten in a lower order form, suitable for a linear finite element approximation by introducing an auxiliary algebraic equation. The additional computational expense of solving this equation is reduced by approximating it in an explicit form and the overall computational expense is that of solving

a system of two coupled partial differential equations, which is the same as for the finite difference methods.

The remainder of this paper is structured as follows. Section 2 describes the chosen mathematical model for shallow water flow. Section 3 reviews a published finite difference method for these equations and proposes a linear finite element method for the spatial approximation coupled with a sophisticated adaptive time integration strategy. In Section 4 the spatial accuracy of the new scheme is analysed by examining the truncation error at a node. In Section 5 numerical experiments are presented comparing the proposed method with theoretical results, experimental results and a previously published finite difference method. Section 6 discusses the results and considers the issues involved in extending this method to two dimensions.

2. THE BOUSSINESQ EQUATION SYSTEM

The physical system can be characterised by a typical water depth H , a typical wavelength λ and a typical wave amplitude a . The non-linearity and dispersion present in the system are parameterised by the ratios ϵ and σ respectively. Ursell [18] discovered a correlation between these two parameters that predicts which wave theory will be applicable. This is known as the Ursell number, U .

$$\epsilon = \frac{a}{H}, \quad (1)$$

$$\sigma = \frac{H}{\lambda}, \quad (2)$$

$$U = \frac{\epsilon}{\sigma^2} = \frac{a\lambda^2}{H^3}. \quad (3)$$

The Boussinesq wave theory requires $\epsilon \ll 1$, $\sigma \ll 1$ and U to be $\mathcal{O}(1)$. The equation system can be consistently derived from the inviscid, incompressible, irrotational fluid flow equations by suitably scaling and non-dimensionalising the equations, integrating through the depth and then expanding in terms of the small parameters σ and ϵ [19]. Terms up to and including $\mathcal{O}(\epsilon, \sigma^2)$ are retained.

Nwogu's extended Boussinesq equation system is given below in terms of free surface elevation $\xi(x, t)$, velocity $u(x, t)$ at depth z , and depth profile $h(x)$,

$$\frac{\partial \xi}{\partial t} + \frac{\partial}{\partial x} ((\xi + h)u) + \frac{\partial}{\partial x} \left(A_1 h^3 \frac{\partial^2 u}{\partial x^2} + A_2 h^2 \frac{\partial^2}{\partial x^2} (hu) \right) = 0, \quad (4)$$

$$\frac{\partial u}{\partial t} + \frac{\partial}{\partial x} \left(\frac{u^2}{2} + g\xi \right) + B_1 h^2 \frac{\partial^3 u}{\partial x^2 \partial t} + B_2 h \frac{\partial^2}{\partial x^2} \left(h \frac{\partial u}{\partial t} \right) = 0, \quad (5)$$

where

$$A_1 = \frac{\theta^2}{2} - \frac{1}{6}, \quad (6)$$

$$A_2 = \theta + \frac{1}{2}, \quad (7)$$

$$B_1 = \frac{\theta^2}{2}, \quad (8)$$

$$B_2 = \theta. \quad (9)$$

The free parameter $\theta = z/h$ is chosen to minimise the difference between the equations' linearised dispersion characteristics and the full linear dispersion relation. A more detailed discussion of this choice is given in References [9,11]. The value $\theta = -0.531$, suggested by Nwogu [9], is used throughout this work.

3. NUMERICAL METHODS

3.1. A finite difference method

Wei and Kirby [11] proposed differencing selected terms of Nwogu's extended system to higher order. They showed that if the first spatial derivative is approximated to fourth-order-accuracy, with the other derivatives approximated to second-order-accuracy, then no non-physical dispersion is produced by the numerical scheme. For the analysis of this scheme, and for comparison with the finite element scheme described and analysed in the following sections, it is helpful to state the form of this discretisation with the leading truncation error terms. On a uniform mesh of size Δ ,

$$\frac{df}{dx}(x_i) = \frac{1}{12\Delta}(f_{i-2} - 8f_{i-1} + 8f_{i+1} - f_{i+2}) - \frac{1}{90}\Delta^4 \frac{d^5f}{dx^5}(x_i) + \mathcal{O}(\Delta^6), \quad (10)$$

$$\frac{d^2f}{dx^2}(x_i) = \frac{1}{\Delta^2}(f_{i-1} - 2f_i + f_{i+1}) + \frac{1}{12}\Delta^2 \frac{d^4f}{dx^4}(x_i) + \mathcal{O}(\Delta^4), \quad (11)$$

$$\frac{d^3f}{dx^3}(x_i) = \frac{1}{2\Delta^3}(-f_{i-2} + 2f_{i-1} - 2f_{i+1} + f_{i+2}) + \frac{7}{60}\Delta^2 \frac{d^5f}{dx^5}(x_i) + \mathcal{O}(\Delta^4). \quad (12)$$

The difference stencils are all centred, to maintain high accuracy. No attempt is made to modify the first derivative stencil to account for convection, as this would introduce diffusive errors in the form of second-order derivatives.

Applying these to Nwogu's system (4)–(5), all the spatial truncation error terms are expressed in terms of fourth and higher derivatives and will not contaminate the real dispersive terms which are at most third-order derivatives in space. In the scaled, non-dimensionalised Boussinesq system [9] these higher derivatives can be neglected as being higher order terms in ϵ and σ without affecting the model. However this scheme remains essentially second-order-accurate in space. The results presented by Wei and Kirby [11] and other work with the same scheme [20] confirm that this finite difference method is both accurate and efficient.

3.2. A finite element method

The third-order spatial derivative present in Equation (4) complicates the application of a finite element method. A weighted residual form of the problem will contain second-order spatial derivatives, and so the usual C^0 finite element approximation cannot be used [17]. Higher order finite element approximations such as the C^1 Hermite cubic and the C^2 cubic spline can be used, but their application is generally limited to regular grids in one dimension [21].

At the expense of introducing an extra equation for a new variable w into the system, the order of the highest spatial derivatives can be reduced:

$$\frac{\partial \xi}{\partial t} + \frac{\partial}{\partial x} ((\xi + h)u) + \frac{\partial w}{\partial x} = 0, \quad (13)$$

$$\frac{\partial u}{\partial t} + \frac{\partial}{\partial x} \left(\frac{u^2}{2} + g\xi \right) + B_1 h^2 \frac{\partial^3 u}{\partial x^2 \partial t} + B_2 h \frac{\partial^2}{\partial x^2} \left(h \frac{\partial u}{\partial t} \right) = 0, \quad (14)$$

$$w - A_1 h^3 \frac{\partial^2 u}{\partial x^2} - A_2 h^2 \frac{\partial^2}{\partial x^2} (hu) = 0. \quad (15)$$

This manipulation of the equation system extends naturally to Nwogu's two-dimensional extended Boussinesq system, where two extra equations must be introduced. The equivalent manipulation of Beji and Nadaoka's equations [8] is not so straightforward when extended to the variable depth case and it is for this reason that Nwogu's system is preferred.

To simplify what follows, the constant depth equations will be used. The finite element method described will apply equally well to the more general system (13)–(15).

$$\xi + \frac{\partial}{\partial x} (p + w) = 0, \quad (16)$$

$$\dot{u} + \frac{\partial q}{\partial x} + \beta \frac{\partial^2 \dot{u}}{\partial x^2} = 0, \quad (17)$$

$$w - \alpha \frac{\partial^2 u}{\partial x^2} = 0, \quad (18)$$

where

$$\dot{v} = \frac{\partial v}{\partial t}, \quad (19)$$

$$p = (\xi + h)u, \quad (20)$$

$$q = \frac{u^2}{2} + g\xi, \quad (21)$$

$$\alpha = (A_1 + A_2)h^3, \quad (22)$$

$$\beta = (B_1 + B_2)h^2. \quad (23)$$

The Galerkin finite element method, analogous to the centred finite difference method of the previous section, is used here [17]. We define a set of N nodes as the intersection points of $(N-1)$ non-overlapping elements that completely cover the spatial domain Ω . A set of basis functions, $\phi_i(x)$, interpolate nodal values of the unknowns over the elements. The finite element method described below is based on a set of standard linear basis functions,

$$\phi_i(x_j) = \delta_{ij}, \quad i, j = 1, 2, \dots, N, \quad (24)$$

where δ_{ij} is the usual delta function. An unknown function $v(x, t)$ is interpolated over the domain as

$$v(x, t) \approx \phi_j(x)v_j(t). \quad (25)$$

The finite element discretisation is developed by multiplying Equations (16)–(18) by a test function, $\phi_i(x)$, and integrating over the spatial domain Ω . The spatial derivatives are

integrated by parts which introduces integrals on the boundary Γ . The approximation (25) is used to replace the continuous functions. The non-linear terms p and q are interpolated as nodal quantities. This form of approximation is known to be accurate for this class of equations [22], and is found to be crucial for the truncation error analysis of Section 4.

$$M_{ij}\dot{\zeta}_j - C_{ij}(p_j + w_j) + \int_{\Gamma} \phi_i(p + w)n_x \, d\Gamma = 0, \quad (26)$$

$$M_{ij}\dot{u}_j - C_{ij}q_j - \beta K_{ij}\dot{u}_j + \int_{\Gamma} \phi_i\left(q + \beta \frac{\partial \dot{u}}{\partial x}\right)n_x \, d\Gamma = 0, \quad (27)$$

$$M_{ij}w_j + \alpha K_{ij}u_j - \alpha \int_{\Gamma} \phi_i \frac{\partial u}{\partial x} n_x \, d\Gamma = 0, \quad (28)$$

where n_x is the outward normal at the boundary of the one-dimensional domain, and

$$M_{ij} = \int_{\Omega} \phi_i \phi_j \, d\Omega, \quad (29)$$

$$C_{ij} = \int_{\Omega} \frac{d\phi_i}{dx} \phi_j \, d\Omega, \quad (30)$$

$$K_{ij} = \int_{\Omega} \frac{d\phi_i}{dx} \frac{d\phi_j}{dx} \, d\Omega. \quad (31)$$

The integrals (29)–(31) are evaluated by integrating over each element individually and summing the results at the nodes. This procedure is simple to automate using the *isoparametric concept* [17], where the integration on each element is mapped to a unit reference element on which the values (29)–(31) can be precomputed.

Equation (28) represents an additional algebraic system to solve at each time step which will increase the required computational time by approximately one-half over the finite difference schemes, which can directly replace the third spatial derivative. In two dimensions there will be two auxiliary variables and hence two, in general sparse, matrix systems to be solved. The solution of the system (28) requires the inversion of the matrix M , generally termed the *mass matrix* [17]. A considerable simplification is achieved if the mass matrix can be replaced by a purely diagonal approximation, or in the finite element terminology *lumped* [17]. This equation can then be decoupled from the $3N$ -dimensional system (26)–(28) and solved explicitly at each time step. This will make the finite element scheme competitive with existing finite difference spatial discretisations, which produce only a $2N$ -dimensional system of differential equations in time. The lumping procedure replaces Equation (28) with

$$w_i = \frac{1}{M_i^L} \left(-\alpha K_{ij}u_j + \alpha \int_{\Gamma} \phi_i \frac{\partial u}{\partial x} n_x \, d\Gamma \right), \quad (32)$$

where

$$M_i^L = \sum_j M_{ij}. \quad (33)$$

Although lumping the matrix is known to decrease the accuracy of the approximation [17], the analysis in Section 4 shows that the spatial truncation error is not significantly affected by this approximation. An alternative approach to inverting the mass matrix in Equation (28) without the diagonal approximation, would be to use the simple iterative method of Donea and Giuliani [23].

Suitable boundary conditions are required for the numerical experiments. At an inflow boundary the free surface elevation, ξ , is prescribed. For the periodic wave cases considered here, the velocity u and auxiliary variable w are evaluated using the linearised form of equations (16)–(18), and are also prescribed at the inflow points [11]. At an outflow boundary it is important to minimise non-physical reflection of information back into the domain. A simple radiation boundary condition [20] is not completely effective because the dispersive waves have no single phase speed. Here a sponge layer [11] is introduced near the outflow boundary in the form of a viscous term which increases in magnitude closer to the outflow. These viscous terms are added to Equations (26) and (27). The amount of viscosity has to be determined by experiment so as to effectively damp the outgoing waves without allowing significant reflection. At a solid, reflecting boundary the impermeability condition

$$un_x = 0 \quad \Rightarrow \quad u = 0, \quad (34)$$

is prescribed, and from considering Equation (16),

$$\int_{\Omega} \dot{\xi} \, d\Omega = - \int_{\Omega} \frac{\partial}{\partial x} (p + w) \, d\Omega, \quad (35)$$

$$\frac{\partial}{\partial t} \left(\int_{\Omega} \xi \, d\Omega \right) = - \int_{\Gamma} (p + w)n_x \, d\Gamma = 0, \quad (36)$$

by conservation of mass. Therefore at the reflecting boundary, Equation (27) is replaced by Equation (34) and the boundary integral in Equation (26) is set to zero. The boundary integral in Equation (32) is undetermined at outflow and solid boundaries and is extrapolated from the adjacent element in these cases. Partial reflection is not considered here but can be implemented as a simple modification to the fully reflecting boundary conditions [9]. Another important boundary condition is that of wave reflection at the inflow boundary. However this is not relevant to the examples considered here.

3.3. Time integration

Truncation errors from a low-order time integration scheme will also produce non-physical dispersion and contaminate the mathematical model. In previous work the time integration has usually been with a high-order accuracy predictor–corrector method [11,20], or with a lower order method and corrections for the truncation errors [9,10]. In this work we achieve the necessary accuracy by making use of variable order, variable time step software based on backward differentiation formulae (BDF) as implemented in the SPRINT package [16].

The spatial discretisation described in Section 3.2 results in a $2N$ -dimensional linear system of differential equations of the form

$$A_{ij}\dot{y}_j - f_i = 0, \quad (37)$$

where

$$y = (\xi_1, u_1, \xi_2, u_2, \dots, \xi_N, u_N)', \quad (38)$$

$$f = f(t, y). \quad (39)$$

The software controls the local error in y over each time step by varying both the order of the BDF method and the time step, so that a uniformly high accuracy in time can be achieved [24]. The user controls the local error by supplying relative and absolute tolerances, r_{tol} and a_{tol} respectively, which can be vector quantities in general. Here, r_{tol} and a_{tol} are scalar values

determined by experiment; lowering their values until solution independency is established. This will ensure that the error in the solution is dominated by the spatial discretisation error. In this work $r_{\text{tol}} = a_{\text{tol}} = 10^{-6}$ was chosen after repeated experiments, reflecting the high accuracy required in the time integration.

Consistent initial conditions are calculated automatically by the software. Given an initial solution, $y(t_0)$, initial time derivatives, $\dot{y}(t_0)$, are computed such that the system (37) is satisfied [25].

4. TRUNCATION ERROR ANALYSIS

In this section the truncation error of the linear finite element scheme defined by Equations (26), (27) and (32) will be analysed. The linear finite element scheme is only second-order-accurate in space and it is therefore possible that error terms will contaminate the physical dispersion in a similar way to a low-order finite difference method. The analysis that follows will show that this does not happen here and that the truncation error is of a similar form to that of Wei and Kirby's finite difference scheme (10)–(12) described in Section 3.1.

With a linear finite element discretisation on a regular mesh of element length Δ , Equation (27) has the following form at an internal node:

$$\frac{\Delta}{6}(\dot{u}_{i-1} + 4\dot{u}_i + \dot{u}_{i+1}) + \frac{1}{2}(q_{i+1} - q_{i-1}) - \frac{\beta}{\Delta}(-\dot{u}_{i-1} + 2\dot{u}_i - \dot{u}_{i+1}) = 0. \quad (40)$$

Using standard Taylor series expansions in space and the original Equation (27), it is straightforward to show that the truncation error at a node has the form

$$-\beta \frac{\Delta^2}{12} \frac{\partial^4 \dot{u}_i}{\partial x^4} + \Delta^4 \left(\frac{1}{72} \frac{\partial^4 \dot{u}_i}{\partial x^4} + \frac{1}{120} \frac{\partial^5 q_i}{\partial x^5} + \frac{\beta}{360} \frac{\partial^6 \dot{u}_i}{\partial x^6} \right) + \mathcal{O}(\Delta^6). \quad (41)$$

The leading term is $\mathcal{O}(\Delta^2)$ due to the linear approximation but multiplies a fourth-order derivative. This will not corrupt the physical dispersion present in the system, which depends on third and lower derivatives, and suggests that the linear finite element approximation is acceptable for this equation.

With a linear finite element discretisation on a regular mesh of element length Δ , Equations (26) and (32) have the following form at an internal node:

$$\frac{\Delta}{6}(\dot{\xi}_{i-1} + 4\dot{\xi}_i + \dot{\xi}_{i+1}) + \frac{1}{2}(p_{i+1} - p_{i-1}) + \frac{1}{2}(w_{i+1} - w_{i-1}) = 0, \quad (42)$$

$$\Delta w_i + \frac{\alpha}{\Delta}(-u_{i-1} + 2u_i - u_{i+1}) = 0. \quad (43)$$

Again, using Taylor series expansions and then using Equation (43) to replace the w_i terms in Equation (42), the truncation error at a node is

$$\alpha \frac{\Delta^2}{12} \frac{\partial^5 u_i}{\partial x^5} + \Delta^4 \left(\frac{1}{72} \frac{\partial^4 \dot{\xi}_i}{\partial x^4} + \frac{1}{120} \frac{\partial^5 p_i}{\partial x^5} + \frac{\alpha}{40} \frac{\partial^7 u_i}{\partial x^7} \right) + \mathcal{O}(\Delta^6). \quad (44)$$

The leading truncation error term indicates that the discretisation is $\mathcal{O}(\Delta^2)$ accurate but that the form of this leading error will not contaminate the physical dispersion. Importantly, the accuracy does not appear to have been significantly reduced by the diagonal approximation of the mass matrix in Equation (43).

It has been shown that a linear finite element discretisation can produce a suitable numerical model for Nwogu's extended Boussinesq equations. The model is only second-order-accurate, but the form of the leading error terms will not contaminate the physical dispersion present in the equations. This scheme can therefore be thought of as an analogue of Wei and Kirby's finite difference scheme, which approximates the first-order spatial derivatives to higher order, to produce a similar effect. Lumping the mass matrix in Equation (28) considerably improves the efficiency of the scheme, as w can now be calculated without the inversion of a matrix. In two dimensions this saving will be even more significant. This truncation error analysis can be directly extended to the Boussinesq system with non-uniform depth (13)–(15) discretised on a regular mesh.

The proposed finite element method is simple to extend to a non-uniform mesh. However the truncation error analysis of this section has to be modified to account for a varying mesh. For example, if Δ_i denotes the length of the element $[x_i, x_{i+1}]$, the truncation error of Equation (27) can, with some manipulation, be shown to be

$$\left(\frac{\Delta_i - \Delta_{i-1}}{6}\right) \frac{\partial^2 q_i}{\partial x^2} - \frac{1}{12} \left(\frac{\Delta_i^3 + \Delta_{i-1}^3}{\Delta_i + \Delta_{i-1}}\right) \beta \frac{\partial^4 \dot{u}_i}{\partial x^4} + \mathcal{O}(\Delta_{i-1}^3, \Delta_i^3). \quad (45)$$

The leading term will produce numerical diffusion in the scheme. It may be possible to restrict the amount of diffusion present by limiting the rate of variation in the mesh size, i.e. keeping $(\Delta_i - \Delta_{i-1})$ small. An example is included in the following section to illustrate the effect of a non-uniform mesh.

5. NUMERICAL EXPERIMENTS

5.1. A solitary wave with constant depth

The simulation of a solitary wave requires that both the non-linearity and dispersion are accurately modelled. This case is used here to assess the accuracy of the finite element model and the time integration strategy. Wei and Kirby have derived an approximate solitary wave solution of Nwogu's extended Boussinesq system:

$$\xi(x, t) = a_1 \operatorname{sech}^2(b(x - ct)) + a_2 \operatorname{sech}^4(b(x - ct)), \quad (46)$$

$$u(x, t) = a \operatorname{sech}^2(b(x - ct)). \quad (47)$$

The expressions for the coefficients a_1 , a_2 , a , b and c are given in Reference [11]. The spatial domain $x \in [-50, 250]$ is uniformly discretised with 600 linear finite elements and, equivalently, 601 equally spaced finite difference nodes. The spatial domain is infinite theoretically but in practice it is truncated at a suitable distance from the wave and all variables are set to zero at the boundaries. Inflow and outflow boundary conditions are not considered in this example. The wave is initially at the origin and of amplitude 0.045 m, and is propagated for 100 s over an undisturbed depth of 0.45 m. Figure 1 compares the theoretical free surface profile of Equation (46) at $t = 100$ s with the numerical results from both the proposed finite element scheme and the finite difference scheme described in Section 3.1 coupled with the SPRINT time integration. There is an almost identical slight phase error in the numerical results and a small dispersive tail, but in general both methods propagate the solitary wave accurately. The solution (46) is only an approximation for these equations and so an exact agreement is unlikely.

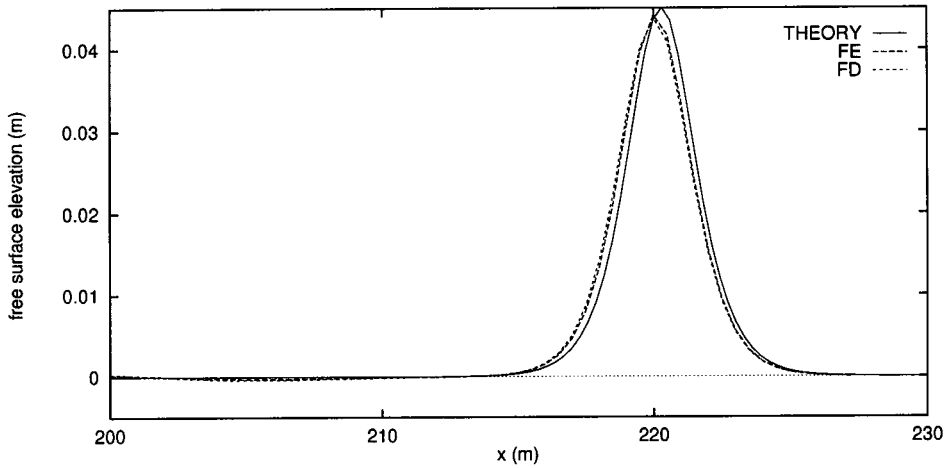


Figure 1. Free surface profile at $t = 100$ s for the constant depth solitary wave.

5.2. A solitary wave propagating up a slope and reflecting from a vertical wall

The depth profile for this problem is shown in Figure 2. Experimental data is available for this problem in the form of time series of the free surface elevation at various locations on the slope [26]. The spatial domain $x \in [-55, 20]$ is uniformly discretised with 600 linear finite elements and the equations are integrated in time for $t \in [0, 30]$ with the wave initially centred at $x = -30$. At $x = -55$ all variables are set to zero and at $x = 20$ the fully reflecting boundary conditions are applied. Figure 3 compares the numerical and experimental time series of the free surface elevation at $x = 17.75$ m for a solitary wave of initial amplitude 0.07 m. The first peak corresponds to the incident wave which is well predicted by the code. The second peak is the reflected wave which is overpredicted by 8%. It is possible that this overprediction is produced because the method is based on inviscid equations, and there are no losses at the reflecting wall. Figure 4 compares the time series at the same location for a

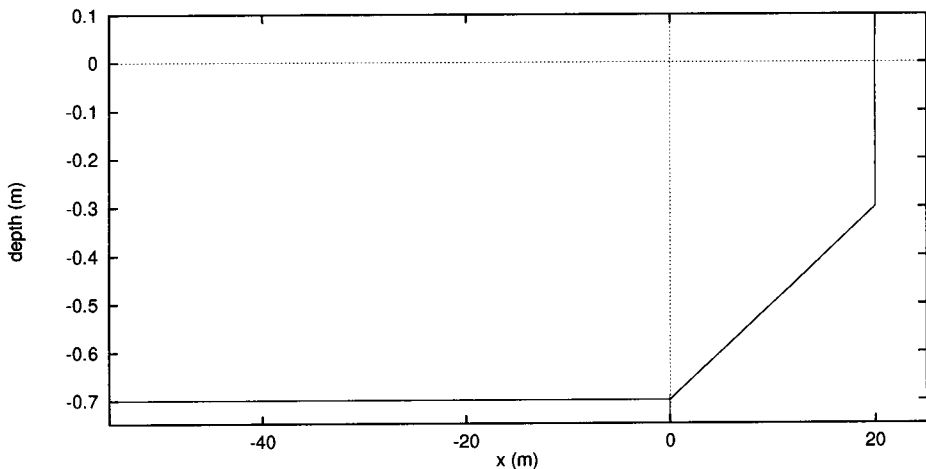


Figure 2. Bathymetry for the solitary wave test cases.

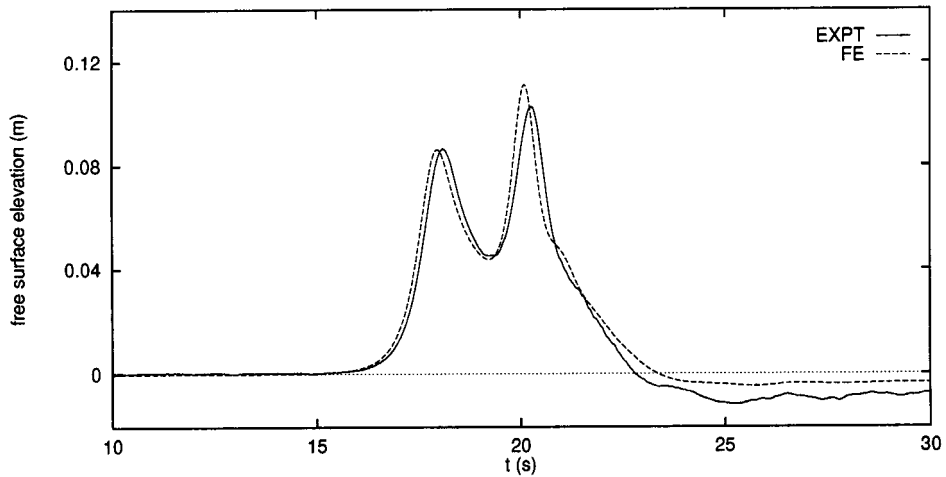


Figure 3. Free surface time history at $x = 17.75$ m for the 0.07 m solitary wave.

solitary wave of larger initial amplitude 0.12 m. In this case the second peak, corresponding to the reflected wave, is overpredicted by 38%. This can be attributed in part to the fact that the extended equations are restricted to weakly non-linear situations, whereas in this case the reflected wave attains an amplitude comparable with the depth at the wall which is clearly outside the range of validity of the Boussinesq theory as stated in Section 2.

5.3. A periodic deep water wave with constant depth

The extended Boussinesq system is able to model wave behaviour right up to the deep water limit $\sigma = 1/2$ [9]. The original Boussinesq equations are not applicable at the deep water limit as their dispersion relation diverges for $\sigma > 0.48$ [9]. The test case is a periodic wave of wavelength $\lambda = 1.12$ m, wave period $\tau = 0.85$ s and amplitude $a = 0.025$ m, propagating into an initially undisturbed region of constant depth $h = 0.56$ m. The incident wave has the form

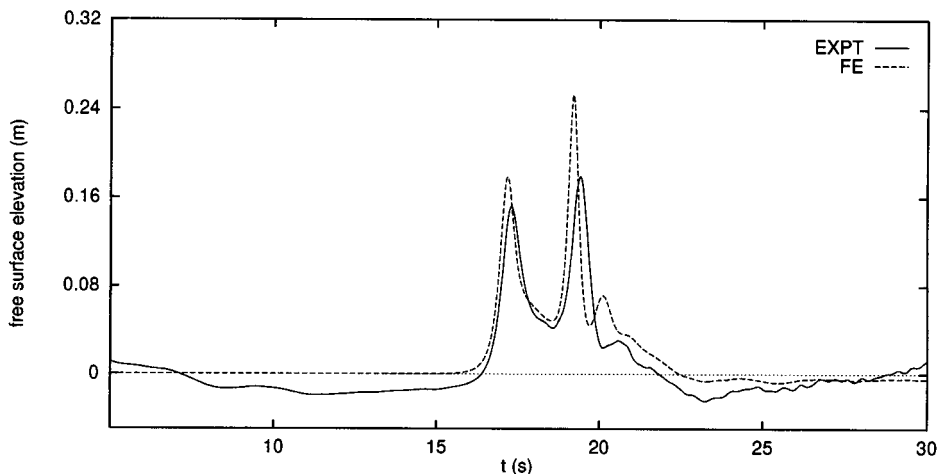


Figure 4. Free surface time history at $x = 17.75$ m for the 0.12 m solitary wave.

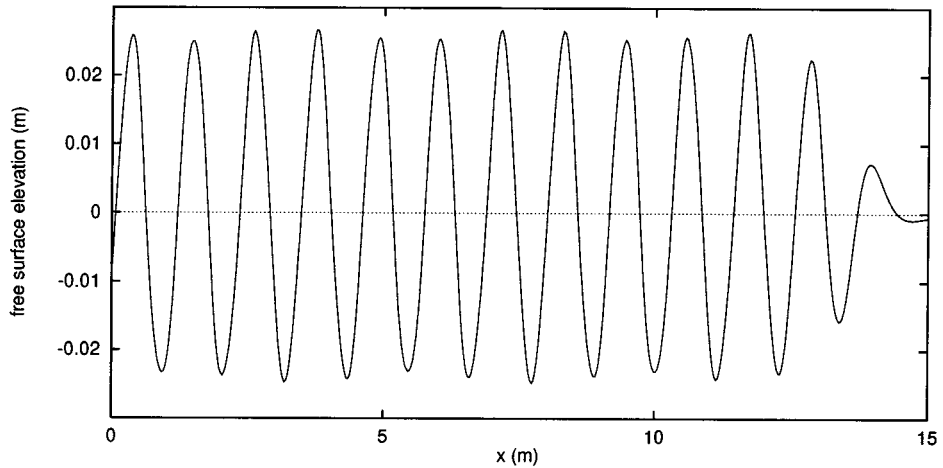


Figure 5. Free surface profile at $t = 40$ s for the deep water wave.

$$\zeta(x, t) = a \sin\left(2\pi\left(\frac{x}{\lambda} - \frac{t}{\tau}\right)\right). \quad (48)$$

The spatial domain $x \in [0, 15]$ is uniformly discretised with 500 linear finite elements and the problem is integrated for $t \in [0, 40]$. The inflow boundary condition is applied at $x = 0$ and a sponge layer is used near the outflow boundary at $x = 15$ to prevent reflection back into the domain. Figure 5 shows the free surface profile at $t = 40$ s. A steady periodic flow has been established and the sponge layer is effectively damping the outgoing wave.

5.4. A periodic wave propagating over a bar

This problem has been studied previously, and experimental data is available for comparison with the numerical results [27]. The depth profile is shown in Figure 6. The input wave is of the form given in Equation (48) with wavelength $\lambda = 3.73$ m, wave period $\tau = 2.02$ s and

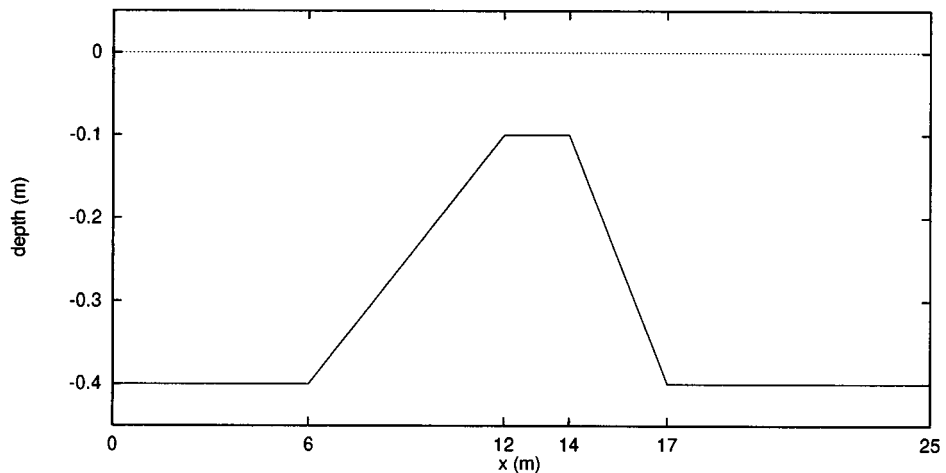


Figure 6. Bathymetry for the bar.

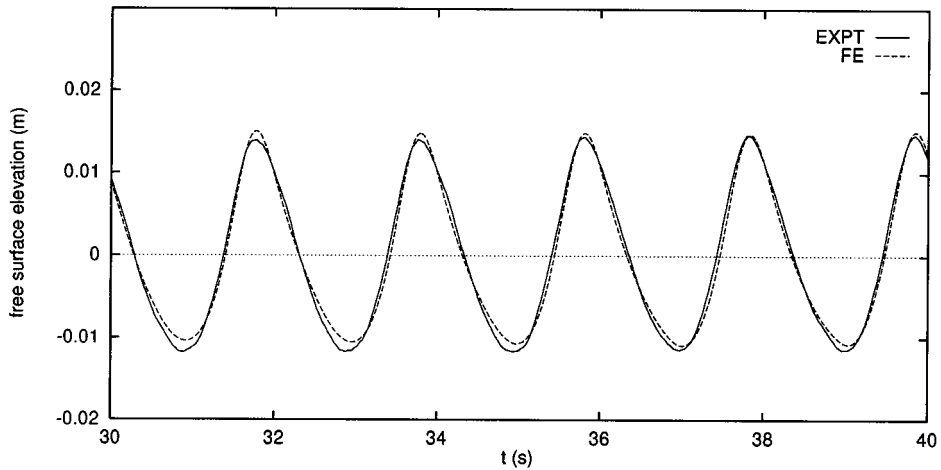


Figure 7. Free surface time history at $x = 10.5$ m.

amplitude $a = 0.01$ m and propagates into an initially undisturbed region of depth $h = 0.40$ m before reaching the bar. A sponge layer is applied at the right boundary to damp the out-going wave. The spatial domain $x \in [0, 25]$ is uniformly discretised with 500 linear finite elements and the problem is integrated in time for $t \in [0, 40]$. Figures 7–9 compare the time histories of the free surface profile with the experimental data at $x = 10.5$, 13.5 and 17.3 m, respectively. A visual comparison of the results with a similar study using a finite difference method [20] shows no significant differences in the graphs.

5.5. A non-uniform mesh

The solitary wave experiment of Section 5.2 is recomputed on a non-uniform grid. The constant depth region $x \in [-55, 0]$ is uniformly discretised as before with 440 linear elements, producing a mesh spacing of 0.125 m. On the slope $x \in [0, 20]$ the mesh spacing is linearly varied from the constant depth value of 0.125 m at the base to 0.036 m at the top of the slope.

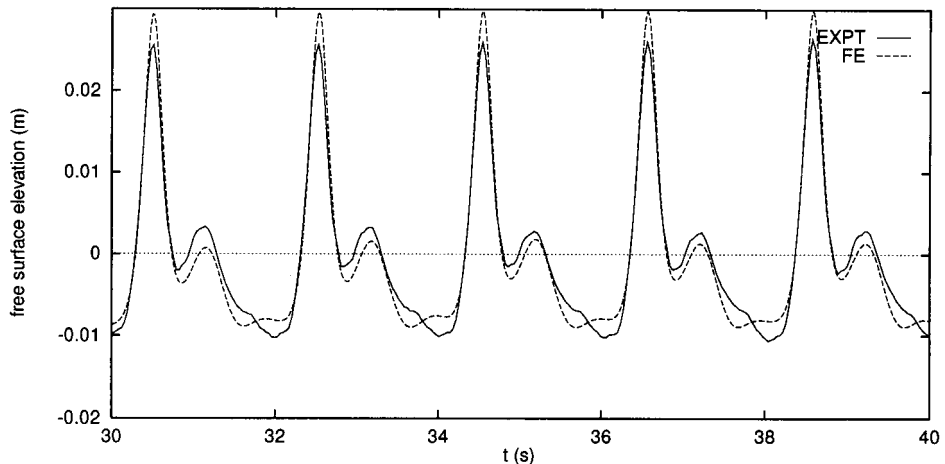


Figure 8. Free surface time history at $x = 13.5$ m.

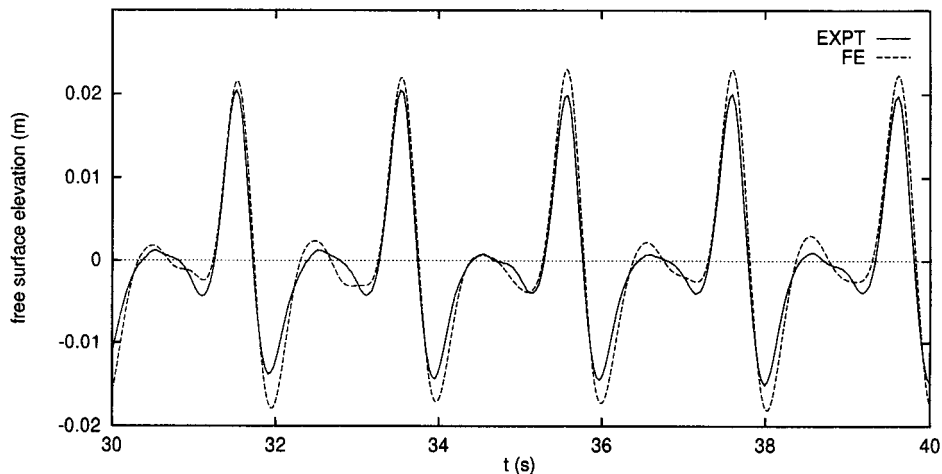


Figure 9. Free surface time history at $x = 17.3$ m.

This allows a better resolution of the wave as it steepens and moves up the slope. The numerical results obtained are graphically indistinguishable from the results presented in Figures 3 and 4. Closer inspection shows the maximum difference between the solutions to be 1.3×10^{-3} or $\approx 1\%$. This suggests that a suitably slow variation in the mesh may not affect the accuracy of the scheme.

6. CONCLUSIONS AND FURTHER WORK

It has been demonstrated both by analysis and by numerical experiments that the proposed linear finite element and adaptive time integration scheme can produce an accurate numerical model for Nwogu's extended Boussinesq system. The solitary wave case in Section 5.1 confirmed the accuracy of the model, and the deep water wave case in Section 5.3 illustrated the improved dispersion characteristics of the extended Boussinesq equations. The model is still limited to weakly non-linear situations, and the high solitary wave case in Section 5.2 showed that model becomes significantly inaccurate as non-linearity increases.

Most importantly this finite element scheme can be extended easily into two dimensions. The two-dimensional equations [9] can be written in a form similar to Equations (13)–(15) by introducing two auxiliary variables. The use of a lumped mass matrix for these two auxiliary equations will make the computational cost of the finite element method comparable with existing finite difference schemes. The truncation error analysis of the one-dimensional system in Section 4 depended on the non-linear terms being written in the compact forms (20) and (21). An equivalent form has been found for the two-dimensional equations. The truncation error analysis suggests that good results may be expected on regular two-dimensional grids and that if the variation of the mesh is suitably controlled that the method will extend successfully to unstructured triangular grids. The two-dimensional model is currently being developed and will be the subject of a further paper.

ACKNOWLEDGMENTS

The authors would like to thank the EPSRC and HR Wallingford for funding in the form of a CASE studentship for MW. The authors also thank A.J. Cooper, J.V. Smallman, J. Lawson and N. Dodd at HR Wallingford for stimulating discussions relating to the work, and for providing the experimental data.

REFERENCES

1. G.B. Whitham, *Linear and Nonlinear Waves*, Wiley-Interscience, New York, 1974.
2. M.B. Abbot, H.M. Petersen and O. Skovgaard, 'On the numerical modelling of short waves in shallow water', *J. Hydraul. Res.*, **16**, 173–203 (1978).
3. A. Schröter, R. Mayerle, A. Kahlfeld and W. Zielke, 'Assessment of a Boussinesq wave model for the design of a harbour', in *International Conference on Coastal and Port Engineering in Developing Countries*, 1995, pp. 741–753.
4. O. Nwogu, 'Nonlinear transformation of multi-directional waves in water of variable depth', Draft manuscript, 1993.
5. D.H. Peregrine, 'Long waves on a beach', *J. Fluid Mech.*, **27**, 815–827 (1967).
6. P.A. Madsen, R. Murray and O.R. Sørensen, 'A new form of the Boussinesq equations with improved linear dispersion characteristics', *Coast. Eng.*, **15**, 371–388 (1991).
7. P.A. Madsen and O.R. Sørensen, 'A new form of the Boussinesq equations with improved linear dispersion characteristics. Part 2. A slowly varying bathymetry', *Coast. Eng.*, **18**, 183–204 (1992).
8. S. Beji and K. Nadaoka, 'A formal derivation and numerical modelling of the improved Boussinesq equations for varying depth', *Ocean Eng.*, **23**, 691–704 (1996).
9. O. Nwogu, 'Alternative form of Boussinesq equations for nearshore wave propagation', *ASCE J. Waterw., Port, Coast., Ocean Eng.*, **119**, 618–638 (1993).
10. M.B. Abbot, A.D. McCowan and I.R. Warren, 'Accuracy of short-wave numerical models', *ASCE J. Hydraul. Eng.*, **110**, 1287–1301 (1984).
11. G. Wei and J.T. Kirby, 'Time-dependent numerical code for extended Boussinesq equations', *ASCE J. Waterw., Port, Coast., Ocean Eng.*, **121**, 251–261 (1995).
12. J.S. Antunes do Carmo, F.J. Seabra Santos and E. Barthélemy, 'Surface waves propagation in shallow water: a finite element model', *Int. J. Numer. Methods Fluids*, **16**, 447–459 (1993).
13. N.D. Katopodes and C. Wu, 'Computation of finite-amplitude dispersive waves', *ASCE J. Waterw., Port, Coast., Ocean Eng.*, **113**, 327–346 (1987).
14. M. Kawahara and J.Y. Cheng, 'Finite element method for Boussinesq wave analysis', *Int. J. Comput. Fluid Dyn.*, **2**, 1–17 (1994).
15. M. Dæhlen and A. Tveito (eds), *Numerical Methods and Software Tools in Industrial Mathematics*, Birkhäuser, Boston, 1997.
16. M. Berzins, P.M. Dew and R.M. Furzeland, 'Developing software for time-dependent problems using the method of lines and differential-algebraic integrators', *Appl. Numer. Math.*, **5**, 375–397 (1989).
17. O.C. Zienkiewicz and K. Morgan, *Finite Elements and Approximation*, Wiley-Interscience, New York, 1983.
18. F. Ursell, 'The long-wave paradox in the theory of gravity waves', *Proc. Cambridge Philosophical Society*, **49**, 685–694 (1953).
19. D.H. Peregrine, 'Equations for water waves and the approximations behind them', in R. Meyer (ed.), *Waves on Beaches and Resulting Sediment Transport*, Academic Press, New York, 1972, pp. 95–122.
20. J. Zang, J. Lawson, N. Tozer and N. Dodd, 'The development of a computational wave model based on extended Boussinesq equations', *Technical report*, HR Wallingford, 1996.
21. G. Strang and G.J. Fix, *An Analysis of the Finite Element Method*, Prentice-Hall, Englewood Cliffs, NJ, 1973.
22. I. Christie, D.F. Griffiths, A.R. Mitchell and J.M. Sanz-Serna, 'Product approximation for non-linear problems in the finite element method', *IMA J. Numer. Anal.*, **1**, 253–266 (1981).
23. J. Donea and S. Giuliani, 'A simple method to generate high-order accurate convection operators for explicit schemes based on linear finite elements', *Int. J. Numer. Methods Fluids*, **1**, 63–79 (1981).
24. M. Berzins, 'Balancing space and time errors in the method of lines for parabolic equations', *SIAM J. Sci. Stat. Comput.*, **12**, 573–594 (1991).
25. M. Berzins and R.M. Furzeland, 'A user's manual for SPRINT—a versatile software package for solving systems of algebraic, ordinary and partial differential equations: part 1—algebraic and ordinary differential equations', *Technical Report TNER.85.058*, Thornton Research Centre, Chester, 1985.
26. N. Dodd, 'A numerical model of wave run-up, overtopping and regeneration', *ASCE J. Waterw., Port, Coast., Ocean Eng.*, 1997. To appear.
27. M.W. Dingemans, 'Comparison of computations with Boussinesq-like models and laboratory measurements', *Technical Report H1684.12*, MAST G8M Coastal Morphodynamics Research Programme, 1994.